Preparation and Characterization of Myristic-palmitic Acid/Nano Silicon Dioxide/Nano Silicon Carbide Composite Phase Change Materials for Air Conditioning Condensation Heat Recovery System

Yanghua CHEN *, Xue YANG, Piaopiao HUANG

School of Advanced Manufacturing, Nanchang University, Nanchang 330031, No.999 Xuefu Road, Honggutan New District, Nanchang City, Jiangxi Province, China

crossref http://dx.doi.org/10.5755/j02.ms.29761

Received XX June 201X; accepted 2 December 201X

In this research, myristic-palmitic acid(MA-PA)/ nano silicon dioxide(nano-SiO_2) was modified by adding nano silicon carbide(nano-SiC) with high thermal conductivity. The MA-PA/nano-SiO_2 composite phase change material (PCM) was prepared by impregnating the MA-PA eutectic mixture as PCM into nano-SiO_2 as supporting material. Nano- SiC was added to improve the thermal conductivity of MA-PA/nano-SiO_2 composite PCM. Leakage experiments demonstrated that the optimal percentage of MA-PA eutectic mixture adsorbed in nano-SiO_2 was 62wt%. The results of thermal conductivity meter measurement showed that the heat transfer coefficient of the MA-PA/nano-SiO_2 /nano- SiC composite PCM with 9wt% nano-SiC was 0.776 W/(mK), which increased by 83.02% compared with MA-PA/nano-SiO_2 composite PCM. The composite PCM melted at 42.96°C with a latent heat of 88.37J/g and solidified at 44.12°C with a latent heat of 82.45J/g, which were examined by using the differential scanning calorimeter. Thermogravimetric analyzer test results find that composite PCMs had good thermal stability in the working temperature range. Based on the above results, it was known that modified MA-PA/nano-SiO_2 /nano- SiC composite PCMs had better thermodynamic properties and were widely applied future in air conditioning condensation heat recovery systems.

Keywords: composite phase change material; nano silicon dioxide; nano silicon carbide; air conditioning condensation heat recovery system.

1. INTRODUCTION

Energy storage technology, as the focus of recent research in the field of energy applications, can effectively alleviate the energy crisis caused by rapid industrial development. PCMs, as an energy storage medium, can store or release energy at an almost constant temperature during melting or solidification [1]. PCMs have good heat storage performance and can effectively adjust the continuity and periodicity of energy utilization in practical applications. Meanwhile, PCMs plays a role in peak shift adjustment and improve energy efficiency. At present, there are important development prospects in the application area of building energy saving [2], solar energy [3], and waste heat recovery [4]. At present, a large number of organic and inorganic PCM had been studied. Among them, the fatty acid in the organic PCM was an important medium in the field of phase change energy storage. It showed good thermal stability, good chemical properties, low cost, and non-toxicity, as well as high latent heat value, little or no supercooling, and small volume change during the phase change[5].

But some shortcomings of fatty acids cannot be ignored. One of its disadvantages is that leakage occurs easily during the phase change process, thereby affecting its service life. To effectively solve this problem, PCM is adsorbed in materials with porous structures (such as diatomaceous earth [6], nano-SiO_2 [7], expanded perlite [8]) to prepare a shape-stable composite material [9]. Wu et al. [10]prepared composite PCMs with different EG content and bulk density, using stearic acid (SA) as the PCM and expanded graphite (EG) as the porous matrix material. The experimental results showed that EG content of 25 wt.% was the optimal parameter without leakage. The composite PCM indicated excellent thermal performance, and the maximum mass loss of SA was less than 0.5 % after the thermal cycle several times. Luo et al. [11] prepared a composite PCM with capric-palmitic-stearic acid (CA-PA-SA) as the PCM and nano-SiO_2 as the support material. The phase change temperature range was 17.16 ℃ – 26 ℃, and the latent heat was 99.43 J/g. The maximum mass of the CA-PA-SA ternary eutectic mixture contained in the composite PCM was 75 %, and no molten CA-PA-SA exuded from the composite PCM. Li et al. [12] used different dibasic fatty acids as the phase change material and diatomite as the matrix material to prepare shape-stabilized composite PCMs. Chen et al. [13] prepared hexadecanol-myristic acid (HD-MA)/AC composite PCMs. The addition of AC effectively prevented the leakage of the HD-MA eutectic mixture.

* Corresponding author. Tel.: +86-13970944938.
E-mail address: *chenyh@ncu.edu.cn* (Y. Chen)

At the same time, another disadvantage of fatty acid is their low thermal conductivity. This will reduce the energy storage efficiency of the PCM, which is not conducive to practical applications. Many researchers usually added fillers with high thermal conductivity to improve the heat transfer efficiency of composite PCMs, such as β-aluminum nitride [14], carbon nanotubes [15], and SiC [16]. Rezaie [17] introduced green synthetic copper nanoparticles into fatty acids to form a shape-stable composite PCM. The composite PCM added with copper nanoparticles showed good thermal conductivity, increasing by at least 77.5 %. Choi [18] added 0.1 vol% of carbon nanotubes, graphite, and graphene to SA, and its thermal conductivity increased by 10.5 %, 21.55 %, and 9.91 %, respectively. Kumaresan [19] dispersed multi-walled carbon nanotubes(MWCNT) in liquid paraffin to prepare nano-enhanced composite PCMs to increase the transfer efficiency. This study showed that when the content of MWCNT was 0.6 vol%, the heat transfer performance of the composite PCM was significantly improved, and the solidification time was shortened by 33.65 %.

In recent years, the application of PCM in air conditioning condensation heat recovery systems had great prospects. Condensation heat was recovered when PCM underwent phase change and domestic hot water was prepared using condensation heat. This can reduce air pollution and greenhouse gas emissions and can also improve the atmospheric environment, which has significant energy saving and environmental protection. In this study, nano-SiO_2 was selected as the porous matrix material because nano-SiO_2 is stable, porous, non-toxic, and non-polluting [20]. Nano-SiC has such properties as wide bandgap and good thermal conductivity [21]. It was a good choice that nano-SiC was used as a modified additive to further improve the heat transfer efficiency. The phase transition temperatures of MA and PA are 54 °C and 62 °C [22], both of which are not suitable for air conditioning condensation heat recovery systems. The ideal phase transition temperature is achieved by preparing MA-PA eutectic mixture. The main goal of this work was to prepare the MA-PA/nano-SiO_2/ nano-SiC composite PCM for air conditioning condensation heat recovery by melt blending with MA-PA eutectic mixture as PCM, nano-SiO_2 as a porous material, and nano-SiC as modified particles. The appropriate phase transition temperature was achieved by preparing the MA-PA eutectic mixture. The MA-PA eutectic mixture was adsorbed to nano-SiO_2 to prevent its leakage, and the thermal conductivity of the composite PCM was enhanced by adding nano-SiC. The microstructure, chemical structure, heat storage performance, thermal conductivity, thermal stability, and reliability of the MA-PA/nano-SiO_2/ nano-SiC composite PCM were analyzed by ESEM, FT-IR, DSC, Hot Disk, and TGA.

2. EXPERIMENTAL

2.1. Materials

Palmitic acid (PA) (purity ≥ 98 %) and myristic acid (MA) (purity ≥ 98 %) were provided from Shanghai Sinopharm Chemical Reagent Co., Ltd. Nano-SiO_2 (500 nm) was purchased from Macleans Biochemical Technology Co., Ltd. Nano-SiC (300 nm) was purchased from Cote New Materials Technology Co., Ltd.

2.2. Preparation of the MA-PA eutectic mixture

As is known to all, the phase transition temperatures of MA and PA were not suitable for air conditioning condensation heat recovery system. Therefore, the phase transition temperature was adjusted to a suitable value by preparing MA-PA eutectic mixture. According to the phase equilibrium theory and the second law of thermodynamics, the Schrader formula can predict the mass ratio and phase transition temperature *T* of the MA-PA eutectic mixture. The Schrader equation is as follows:

$$T = \left(\frac{1}{T_i} - \frac{Rlnx_i}{\Delta H_i}\right)^{-1} (i = A,\ B), \quad (1)$$

where T_i and ΔH_i represented melting temperature and latent heat of component *i*; x_i was the content of component *i*; *R* was the gas constant. The predicted phase diagrams of MA and PA eutectic systems were shown in Fig. 1. In the next work, the MA-PA eutectic mixture with a mass of 6.5:3.5 was used as the eutectic PCM. MA and PA weighed by mass were continuously stirred in a magnetic stirrer at 70 °C and 800 rpm for 30 minutes, and cooled to room temperature to obtain a eutectic mixture.

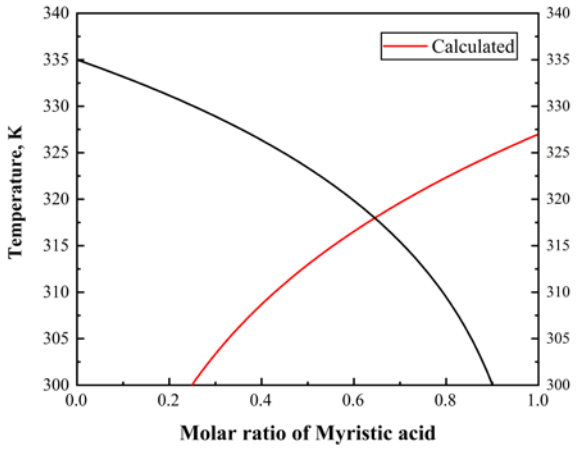

Fig. 1. Melting temperatures of MA-PA mixture versus composition of the components

2.3. Preparation of MA-PA/nano-SiO_2 composite PCM

In this study, 5 groups of composite PCMs with MA-PA eutectic mixture content of 56 wt.%, 59 wt.%, 62 wt.%, 65 wt.%, and 68 wt.% were fabricated to find the best composite ratio without leakage. The specific data of each component were shown in Table 1. Firstly, nano-SiO_2 was spread in absolute ethanol and continuously stirred at 65 °C and 800 rpm for 30 minutes. Then, the MA-PA eutectic mixture was poured into nano-SiO_2 and stirred at 65 °C and 800 rpm until absolute ethanol volatilized completely. Finally, prepared MA-PA/nano-SiO_2 composite PCMs were dried in a blast drying oven at 35 °C for 24 h and named SPCM1, SPCM2, SPCM3, SPCM4, and SPCM5, respectively. The content of PCM determined the latent heat of composite PCM. To maximize the content of the MA-PA

eutectic mixture without leakage, a leakage test was performed on the samples. A proper quantity of composite PCM was put on the white paper and heated at 70 °C for 1 h to test the leakage of different samples.

Fig. 2 showed the results of the leak test. The results showed that when the mass percentage of MA-PA eutectic mixture was 56 wt.%, 59 wt.%, 62 wt.%, there was no oil ring on the white paper, meaning that no leakage had occurred; when the mass percentage of MA-PA eutectic mixture was 65 wt.%, the oil ring can be slightly seen on the white paper, indicating that a small amount of leak; when the mass percentage of the MA-PA eutectic mixture was 69 wt.%, the oil ring can be seen on the white paper, illustrating that a significant leak had occurred. Therefore, the content of the MA-PA eutectic mixture was chosen to be 62 wt.%.

Table 1. Composition of the MA-PA/nano-SiO_2 composite PCMs

Samples	MA-PA, g	Nano-SiO_2, g	Mass fraction of MA-PA, %	Leakage in a molten state
SPCM1	10	7.86	56	No leakage
SPCM2	10	6.59	59	No leakage
SPCM3	10	6.13	62	No leakage
SPCM4	10	5.38	65	Slight leakage
SPCM5	10	4.71	68	Leakage

Table 2. Composition of the MA-PA/nano-SiO_2 /nano-SiC composite PCMs

Samples	SPCM3, g	Nano-SiC, g	Mass fraction of nano-SiC, %
CPCM1	20	0.62	3
CPCM2	20	1.28	6
CPCM3	20	1.99	9

2.4. Preparation of MA-PA/nano-SiO_2/nano-SiC composite PCM

Nano-SiC was added to modify MA-PA/nano-SiO_2 composite PCMs. Three modified composite PCMs containing 3, 6, and 9 wt.% nano-SiC were prepared, denoted as CPCM1, CPCM2, and CPCM3, respectively. The specific data were listed in Table 2. After the mixture of MA-PA eutectic mixture and nano-SiO_2 were stirred at 65 °C and 800 rpm for 30 minutes, nano-SiC was added and stirred at the same temperature and stirring speed until absolute ethanol volatilized completely. Finally, prepared samples were dried in a blast drying oven at 35 °C for 24 h.

2.5. Characterization

The microstructure and chemical microscope of composite PCMs were observed by environmental scanning electron microscope (ESEM, Quanta200FEG). To get a clearer image, all samples were sprayed with gold under blast drying to enhance the conductivity before observation. The chemical structures of composite PCMs, MA-PA eutectic mixture, nano-SiO_2, and nano-SiC were determined by Fourier Transform Infrared Spectrometer (FT-IR, Nicolet570) on a KBr sample chip with a resolution of 2 cm^{-1} and a spectral range of 400 cm^{-1} – 4000 cm^{-1}. The latent heat and phase transition temperature of the composite PCMs and MA-PA eutectic mixture were investigated by differential scanning calorimetry (DSC, DSC 8500, PE, America). The DSC measurement was carried out under a continuous nitrogen flow with a temperature accuracy of 0.2 °C, an enthalpy accuracy of 5 %, a temperature rise and fall rate of 5 °C/min, and a temperature range of 10 – 90 °C. The thermal stability of the composite PCMs was tested by a thermogravimetric analyzer (TGA, TGA4000, PE, America) under continuous nitrogen flow at a heating rate of 20 °C/min from room temperature to 700 °C. At room temperature, a thermal constant thermal conductivity meter (hot disk TPS 2500s) was used to analyze the heat transfer coefficients of different composite PCMs.

3. RESULTS AND DISCUSSION

3.1. Microstructure analysis

The microstructures of nano-SiO_2, nano-SiC, SPCM3, and CPCM1-CPCM3 were determined by ESEM, and the micrographs and presented in Fig. 3.

Fig. 2. Leakage tests of the MA-PA/nano-SiO_2 composites with different MA-PA content

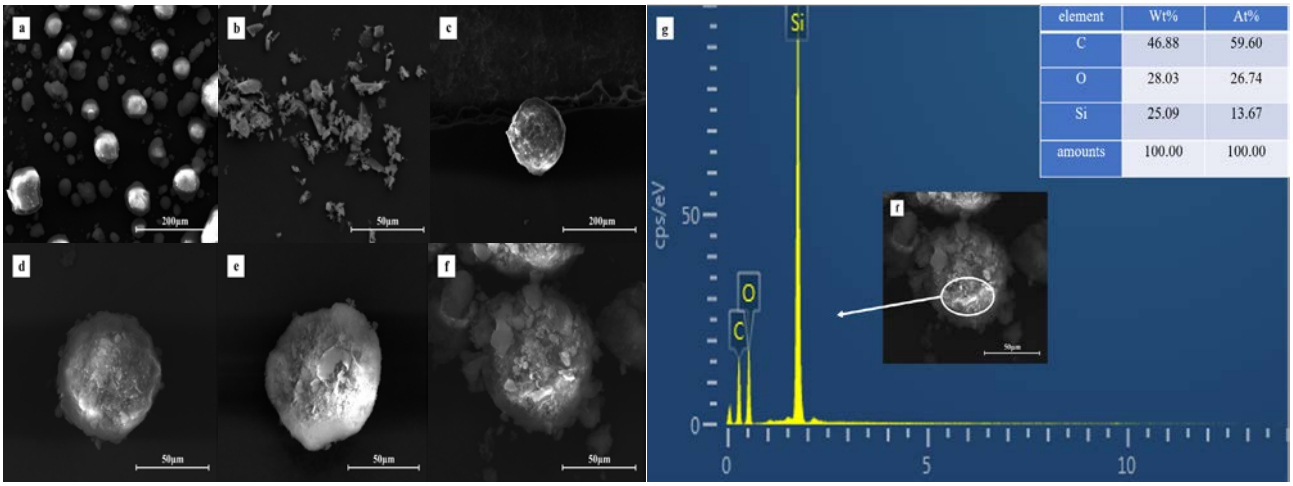

Fig. 3. ESEM photographs of different composite PCMs: a – nano-SiO_2; b – nano-SiC; c – SPCM3; d – CPCM1; e – CPCM2; f – CPCM3 and EDS spectra of CPCM3

It can be seen from Fig. 3 a and b that nano-SiO_2 had a spherical structure and nano-SiC was a flaky structure. Fig. 3 c showed that the MA-PA eutectic mixture uniformly covered the pores and surface of nano-SiO_2 so that the original shape of nano-SiO_2 can no longer be maintained.

The micrographs of composite PCMs with nano-SiC content of 3 %, 6 %, 9 % were shown in Fig. 3 d – f we can see that nano-SiC and nano-SiO_2 were tightly combined. In addition, as the nano-SiC content increased, the nano-SiC on the surface of the composite PCMs also increased. Nano-SiC was similar to 'fins' attached to the spherical composite PCM surface. This led to an increase in the heat exchange area between composite PCMs and the surrounding environment thereby improving the heat exchange efficiency. Fig. 3 g displayed the EDS spectrum of CPCM3 and the atomic percentage data of EDS analysis. The data showed that the mass fractions of C, O, and Si were 46.88 wt.%, 28.03 wt.%, and 25.09 wt.% respectively, which were roughly consistent with the theoretical Si content in the CPCM3 sample. Therefore, it was proved that nano-SiO_2, nano-SiC, and the MA-PA eutectic mixture were well combined together.

3.2. FT-IR analysis

The chemical structure of the composite PCM was characterized by FT-IR. The FT-IR spectra of the MA-PA eutectic mixture, nano-SiC, nano-SiO_2, SPCM3, CPCM3 were shown in Fig. 4.

As for the spectrum of nano-SiC, the 827 cm^{-1} band corresponded to the contraction vibration of C-Si [23]. In the spectrum of nano-SiO_2, the peak at 1098 cm^{-1} represented the stretching vibration of the Si-O-Si group. And the tensile and flexural vibrations of the Si-O group led to the spectral bands of 805 and 457 cm^{-1}, respectively [24].

The spectrum of the MA-PA eutectic mixture showed that the strong peaks of 2917 cm^{-1} and 2840 cm^{-1} were attributed to the stretching vibration of the C-H bond in the $-CH_3$ and $-CH_2$ groups. The stretching vibration absorption peaks of 1700 cm^{-1} and 1470 cm^{-1} were due to the C=O bond and -CH bond [25, 26]. The peak at 1300 cm^{-1} and 944 cm^{-1} signified the in-plane bending vibration and out-of-plane bending vibration of the -OH group, respectively.

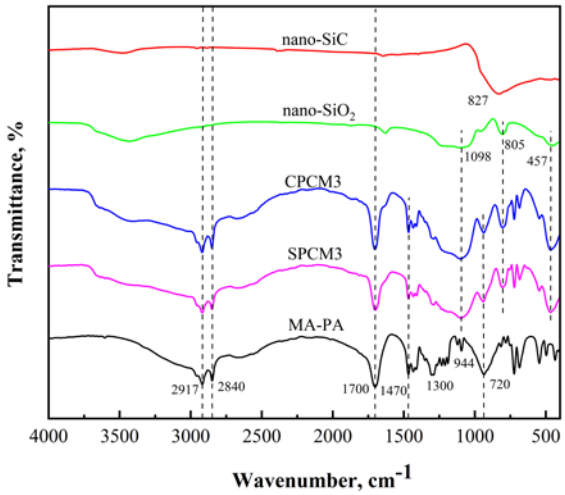

Fig. 4. FT-IR spectra of nano-SiC, nano-SiO_2, MA-PA, SPCM3 and CPCM3

There was an absorption peak at 720 cm^{-1}, which was attributed to the in-plane swinging vibration of the -OH group [27]. It can be found from Fig. 4 that the absorption peaks of $-CH_3$, $-CH_2$, C=O, -OH in the MA-PA eutectic mixture and the absorption peaks of Si-O-Si, Si-O in nano-SiO_2 were all present in CPCM3, which indicated that the MA-PA eutectic mixture successfully absorbed in nano-SiO_2. At the same time, the content of nano-SiC was very small, therefore its absorption peak was almost invisible in CPCM3. The conclusion can be drawn from the above results that the MA-PA, nano-SiO_2, and nano-SiC in the composite PCM are physically combined, not a chemical reaction.

3.3. Thermal property analysis

The phase change latent heat and temperature of the MA-PA eutectic mixture and the prepared composite PCMs were measure by the DSC measurement.

The DSC curves of the MA-PA eutectic mixture and SPCM3, CPCM1, CPCM2, and CPCM3 were presented in Fig. 5. Table 3 contained DSC data such as onset temperature, peak temperature, and latent heat. From the

DSC data of Table 3, the melting/ solidifying temperatures were determined as 48.72/44.49 ℃, 43.01/43.27 ℃, 43.28/43.82 ℃, 43.04/44.29, 42.96/44.12℃ for the MA-PA eutectic mixture, SPCM3 and CPCM1, CPCM2, CPCM3. It was notable that the melting point of composite PCMs became lower than that of the MA-PA eutectic mixture. This result could be attributed to the fact that the composite PCM with high thermal conductivity increased the heat transferred during the melting process, consequently bringing about a decrease in its melting point [28]. The solidifying point of composite PCMs was similar to that of the MA-PA eutectic mixture. It also can be seen that the melting/ solidifying latent heat of SPCM3 and CPCM1, CPCM2, and CPCM3 were 97.12/95.28 J/g, 91.79/86.96 J/g, 90.74/84.89 J/g, 88.37/82.45 J/g respectively, which were lower than that of the MA-PA eutectic mixture (172.42/167.66 J/g). This was because as the content of the MA-PA eutectic mixture which was the only thermal energy storage material decreased, the latent heat value of the composite PCM also decreased correspondingly. Accordingly, the latent heat of the composite PCM can be obtained as:

$$\Delta H_{CPCM} = \eta \cdot \Delta H_{PCM} \ , \quad (2)$$

where η is the mass ratio of the MA-PA eutectic mixture in the composite PCM, ΔH_{CPCM} and ΔH_{PCM} represented the latent heat of composite PCM and the MA-PA eutectic mixture. By comparing the theoretical latent heat, the actual measured latent heat was slightly lower. The reason could be explained that the abnormal interactions between the MA-PA eutectic mixture and the inner surface of the pore of nano-SiO_2 [29]. Table 4 presented the comparison of prepared composite PCM in this study with other composite PCM, which included melting temperature, latent heat, and mass ratio of PCM. It could be concluded that MA-PA/nano-SiO_2/nano-SiC composite PCMs had high latent heat and were suitable phase transition temperatures for air conditioning condensation heat recovery systems. Therefore, this composite PCM has great application prospects.

3.4. Thermal stability analysis

The MA-PA eutectic mixture, nano-SiO_2, SPCM3, and CPCM1-CPCM3 were characterized by TGA and DTG to evaluate the thermal stability. The following figures were TGA (Fig. 6) and DTG (Fig. 7) of all samples. Table 5 collected the temperature T_{peak} of the maximum decomposition rate of the samples and the residual amount at 700 ℃.

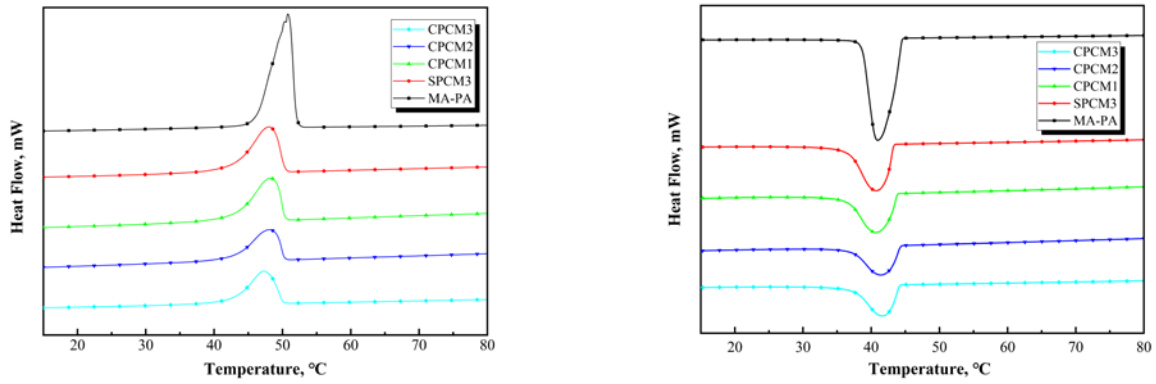

a b

Fig. 5. a – melting DSC curves; b – solidifying DSC curves of MA-PA, SPCM3, CPCM1, CPCM2 and CPCM3

Table 3. DSC data of MA-PA, SPCM3 and composite PCMs with different nano-SiC content

Samples	Melting			Solidifying		
	Onset temperature, ℃	Peak temperature, ℃	Latent heat, J/g	Onset temperature, ℃	Peak temperature, ℃	Latent heat, J/g
MA-PA	48.72	50.79	172.42	44.49	40.95	167.66
SPCM3	43.01	48.00	97.12	43.27	40.72	95.28
CPCM1	43.28	48.20	91.79	43.82	40.70	86.96
CPCM2	43.04	48.05	90.74	44.29	41.44	84.89
CPCM3	42.96	47.27	88.37	44.12	41.66	82.45

Table 4. Comparison of the present work with results of other composite PCM in literature

Composite PCM	Melting temperature, ℃	Melting latent heat, J/g	PCM ratio, %	References
Lauric acid/expanded perlite	44.13	93.36	60.00	[30]
Paraffin/diatomite	41.11	70.51	47.4	[31]
Stearic acid/silica	58.8	82.53	47.6	[32]
Paraffin/montmorillonite	23.1	51.8	60	[33]
MA/polystyrene	47.5	98.26	66.6	[34]
Capric-myristic-stearic acid eutectic mixture/modified expanded vermiculite	22.92	86.4	66.6	[35]
MA-PA/nano-SiO_2/nano-SiC	42.96	88.37	62	Present study

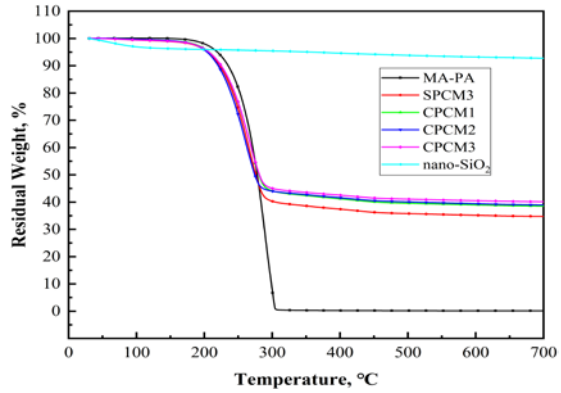

Fig. 6. TGA curves of MA-PA, nano-SiO_2, SPCM3, CPCM1, CPCM2 and CPCM3

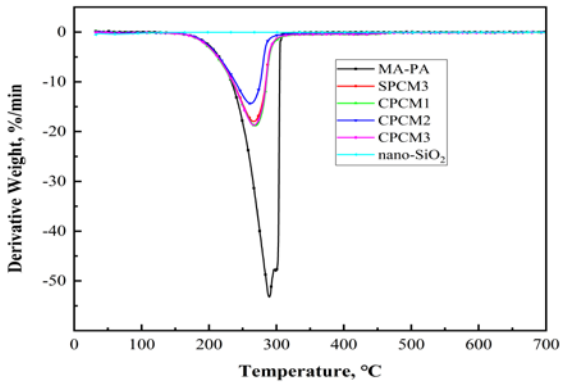

Fig. 7. DTG curves of MA-PA, nano SiO_2, SPCM3, CPCM1, CPCM2 and CPCM3

Table 5. TGA data for MA-PA, nano SiO_2, SPCM3, CPCM1, CPCM2 and CPCM3

Samples	T_{peak}, ℃	Residue, %
MA-PA	289.51	0
Nano-SiO_2	–	92.78
FPCM3	266.37	34.75
CPCM1	268.60	38.49
CPCM2	262.54	39.10
CPCM3	267.01	40.15

As seen in Fig. 6, the weight loss of the MA-PA eutectic mixture in the range of 130 ℃ to 300 ℃ showed only one thermal decomposition with T_{peak} = 289.5 ℃, finally decomposed completely at 300 ℃. The weight loss of nano-SiO_2 was negligible, only 7.22 wt.%, corresponding to the evaporation of water molecules in nano-SiO_2.

Similar to the thermal decomposition process of the MA-PA eutectic mixture, all samples had only one thermal decomposition stage. It was worth noting that the composite PCMs had a faster decomposition rate before 210 ℃ compared to the MA-PA eutectic mixture. This may be because the loose particle state increased the decomposition of the MA-PA eutectic mixture [16]. The working temperature of the prepared composite PCMs was about 43 ℃. At this temperature, the mass loss of composite PCMs was less than 0.03 %. In addition, the decomposition temperature of composite PCMs exceeded 150 ℃, which was much higher than their working temperature. These conclusions can indicate that the prepared composite PCMs had good thermal stability at working temperature.

3.5. Thermal conductivity analysis

The low thermal conductivity of MA-PA/nano-SiO_2 composite PCMs cannot meet the requirements of practical applications, so nano-SiC was added to improve the thermal conductivity of the composite PCM. The thermal conductivity of SPCM3 and CPCM1-CPCM3 was analyzed by Hot Disk. The changing trend of the thermal conductivity of the composite PCM with different nano-SiC contents was presented in Fig. 8.

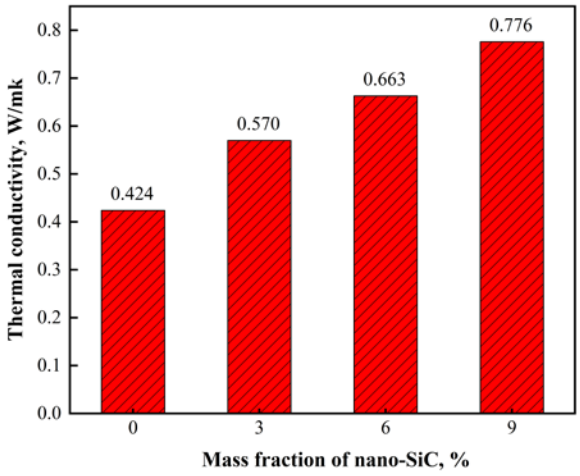

Fig. 8. Thermal conductivity of different composite PCMs

It can be found that the thermal conductivity of the MA-PA/nano-SiO_2 composite PCM without adding nano-SiC was only 0.424 W/mK. After adding 3 wt.% nano-SiC, the thermal conductivity of CPCM1 was 0.570 W/mK, which was 34.4 % higher than that of the composite PCM without adding nano-SiC. After adding more nano-SiC, the thermal conductivity of the composite PCM further increased. The thermal conductivity of CPCM2 with 6 wt.% nano-SiC and CPCM3 with 9 wt.% nano-SiC reached 0.663 W/mK and 0.773 W/mK, which was 56.45 % and 83.02 % higher than that of the composite PCM without nano-SiC.

4. CONCLUSIONS

In this paper, the shape-stable composite PCMs of MA-PA/nano-SiO_2/nano-SiC were prepared which could use in air conditioning condensation heat recovery systems. According to the leakage experiment, it was found that the optimal percentage of the MA-PA adsorbed in nano-SiO_2 was 62wt% without leakage, even in the molten state. The thermal conductivity of composite PCMs was significantly improved after adding nano-SiC. CPCM3 was the best comprehensive performance among all samples, whose melting and solidification temperatures were 42.96 ℃ and 44.12 ℃, and the latent heat of melting and solidification were 88.37 J/g and 82.45 J/g, respectively. Compared with the composite PCM without nano-SiC, the thermal conductivity of CPCM3 was improved by 83.02 %. Based on the above conclusions, the prepared MA-PA/nano-SiO_2/nano-SiC composite PCM was new promising

material in the air conditioning condensation heat recovery system.

REFERENCES

1. **Wang, W., Tang, B., Ju, B., Gao, Z., Xiu, J., Zhang, S.** Fe_3O_4-functionalized Graphene Nanosheet Embedded Phase Change Material Composites: Efficient Magnetic- and Sunlight-Driven Energy Conversion and Storage *Journal of Materials Chemistry A* 5 (3) 2017: pp. 958 – 968. http://dx.doi.org/10.1039/c6ta07144a
2. **Cerón, I., Neila, J., Khayet, M.** Experimental Tile with Phase Change Materials (PCM) for Building Use *Energy and Buildings* 43 (8) 2011: pp. 1869 – 1874. http://dx.doi.org/10.1016/j.enbuild.2011.03.031
3. **Liu, J., Chen, L., Fang, X., Zhang, Z.** Preparation of Graphite Nanoparticles-modified Phase Change Microcapsules and Their Dispersed Slurry for Direct Absorption Solar Collectors *Solar Energy Materials and Solar Cells* 159 2017: pp. 159 – 166. http://dx.doi.org/10.1016/j.solmat.2016.09.020
4. **Gu, Z., Liu, H., Li, Y.** Thermal Energy Recovery of Air Conditioning System—Heat Recovery System Calculation and Phase Change Materials Development *Applied Thermal Engineering* 24 (17 – 18) 2004: pp. 2511 – 2526. http://dx.doi.org/10.1016/j.applthermaleng.2004.03.017
5. **Yuan, Y., Zhang, N., Tao, W., Cao, X., He, Y.** Fatty Acids as Phase Change Materials: A Review *Renewable and Sustainable Energy Reviews* 29 2014: pp. 482 – 498. http://dx.doi.org/10.1016/j.rser.2013.08.107
6. **Wen, R., Zhang, X., Huang, Z., Fang, M., Liu Y., Wu, X., Min, X., Gao, W., Huang, S.** Preparation and Thermal Properties of Fatty Acid/Diatomite Form-stable Composite Phase Change Material for Thermal Energy Storage *Solar Energy Materials and Solar Cells* 178 2018: pp. 273 – 279. http://dx.doi.org/10.1016/j.solmat.2018.01.032
7. **Li, X., Chen, H., Li, H., Liu, L., Lu, Z., Zhang, T., Duan, W. H.** Integration of Form-stable Paraffin/Nanosilica Phase Change Material Composites into Vacuum Insulation Panels for Thermal Energy Storage *Applied Energy* 159 2015: pp. 601 – 609. http://dx.doi.org/10.1016/j.apenergy.2015.09.031
8. **Karaipekli, A., Biçer, A., Sarı, A., Tyagi, V. V.** Thermal Characteristics of Expanded Perlite/Paraffin Composite Phase Change Material with Enhanced Thermal Conductivity Using Carbon Nanotubes *Energy Conversion and Management* 134 2017: pp. 373 – 381. http://dx.doi.org/10.1016/j.enconman.2016.12.053
9. **Zhang, Z., Fang, X.** Study on Paraffin/Expanded Graphite Composite Phase Change Thermal Energy Storage Material *Energy Conversion and Management* 47 (3) 2006: pp. 303 – 310. http://dx.doi.org/10.1016/j.enconman.2005.03.004
10. **Wu, S., Li, T. X., Yan, T., Dai, Y. J., Wang, R. Z.** High Performance Form-stable Expanded Graphite/Stearic Acid Composite Phase Change Material for Modular Thermal Energy Storage *International Journal of Heat and Mass Transfer* 102 2016: pp. 733 – 744. http://dx.doi.org/10.1016/j.ijheatmasstransfer.2016.06.066
11. **Luo, Z., Zhang, H., Gao, X., Xu, T., Fang, Y., Zhang, Z.** Fabrication and Characterization of Form-stable Capric-Palmitic-Stearic Acid Ternary Eutectic Mixture/Nano-SiO_2 Composite Phase Change Material *Energy and Buildings* 147 2017: pp. 41 – 46. http://dx.doi.org/10.1016/j.enbuild.2017.04.005
12. **Li, M., Wu, Z., Kao, H.** Study on Preparation and Thermal Properties of Binary Fatty Acid/Diatomite Shape-stabilized Phase Change Materials *Solar Energy Materials and Solar Cells* 95 (8) 2011: pp. 2412 – 2416. http://dx.doi.org/10.1016/j.solmat.2011.04.017
13. **Chen, Y., Wang, Z., Ge, M., Zhao, F.** Preparation and Thermal Properties of Hexadecanol-Myristic Acid Eutectics/ Activated Carbon Composites as Shape-stabilized Phase Change Materials in Thermal Energy Storage *Materials Science* 27 (4) 2021: pp. 437 – 443. http://dx.doi.org/10.5755/j02.ms.24883
14. **Wang, W., Yang, X., Fang, Y., Ding, J., Yan, J.** Enhanced Thermal Conductivity and Thermal Performance of Form-stable Composite Phase Change Materials by Using B-Aluminum Nitride *Applied Energy* 86 (7 – 8) 2009: pp. 1196 – 1200. http://dx.doi.org/10.1016/j.apenergy.2008.10.020
15. **Biercuk, M. J., Llaguno, M. C., Radosavljevic, M., Hyun, J. K., Johnson, A. T., Fischer, J. E.** Carbon Nanotube Composites for Thermal Management *Applied Physics Letters* 80 (15) 2002: pp. 2767 – 2769. http://dx.doi.org/10.1063/1.1469696
16. **Wang, X., Zhang, C., Wang, K., Huang, Y., Chen, Z.** Highly Efficient Photothermal Conversion Capric Acid Phase Change Microcapsule: Silicon Carbide Modified Melamine Urea Formaldehyde *Journal of Colloid and Interface Science* 582(Pt A) 2021: pp. 30 – 40. http://dx.doi.org/10.1016/j.jcis.2020.08.014
17. **Rezaie, A. B., Montazer, M.** One-step Fabrication of Fatty Acids/Nano Copper/Polyester Shape-stable Composite Phase Change Material for Thermal Energy Management and Storage *Applied Energy* 228 2018: pp. 1911 – 1920. http://dx.doi.org/10.1016/j.apenergy.2018.07.041
18. **Choi, D. H., Lee, J., Hong, H., Kang, Y. T.** Thermal Conductivity and Heat Transfer Performance Enhancement of Phase Change Materials (PCM) Containing Carbon Additives for Heat Storage Application *International Journal of Refrigeration* 42 2014: pp. 112 – 120. http://dx.doi.org/10.1016/j.ijrefrig.2014.02.004
19. **Kumaresan, V., Velraj, R., Das, S. K.** The Effect of Carbon Nanotubes in Enhancing the Thermal Transport Properties of PCM during Solidification *Heat and Mass Transfer* 48 (8) 2012: pp. 1345 – 1355. http://dx.doi.org/10.1007/s00231-012-0980-3
20. **Lin, Y., Cong, R., Chen, Y., Fang, G.** Thermal Properties and Characterization of Palmitic Acid/Nano Silicon Dioxide/Graphene Nanoplatelet for Thermal Energy Storage *International Journal of Energy Research* 44 (7) 2020: pp. 5621 – 5633. http://dx.doi.org/10.1002/er.5311
21. **Yuan, W., Yang, X., Zhang, G., Li, X.** A Thermal Conductive Composite Phase Change Material with Enhanced Volume Resistivity by Introducing Silicon Carbide for Battery Thermal Management *Applied Thermal Engineering* 144 2018: pp. 551-557. http://dx.doi.org/10.1016/j.applthermaleng.2018.07.095
22. **He, Y., Zhang, X., Zhang, Y., Song Q., Liao, X.** Utilization of Lauric Acid-Myristic Acid/Expanded Graphite Phase Change Materials to Improve Thermal Properties of Cement Mortar *Energy and Buildings* 133 2016: pp. 547 – 558. http://dx.doi.org/10.1016/j.enbuild.2016.10.016
23. **Gong, S., Cheng, X., Li, Y., Wang, X., Wang, Y., Zhong, H.**

Effect of Nano-Sic on Thermal Properties of Expanded Graphite/1-Octadecanol Composite Materials for Thermal Energy Storage *Powder Technology* 367 2020: pp. 32-39.
http://dx.doi.org/10.1016/j.powtec.2020.03.039

24. **Zhang, X., Zhu, C., Fang, G.** Preparation and Thermal Properties of N-Eicosane/Nano-SiO_2/Expanded Graphite Composite Phase-change Material for Thermal Energy Storage *Materials Chemistry and Physics* 240 2020: pp. 1 – 9.
http://dx.doi.org/10.1016/j.matchemphys.2019.122178
25. **Mehrali, M., Latibari, S. T., Mehrali, M., Indra Mahlia, T. M., Cornelis Metselaar, H. S., Naghavi, M. S., Sadeghinezhad, E., Akhiani, A. R.** Preparation and Characterization of Palmitic Acid/Graphene Nanoplatelets Composite with Remarkable Thermal Conductivity as A Novel Shape-stabilized Phase Change Material *Applied Thermal Engineering* 61 (2) 2013: pp. 633 – 640.
http://dx.doi.org/10.1016/j.applthermaleng.2013.08.035
26. **Xiao, D., Qu, Y., Hu, S., Han, H., Li, Y., Zhai, J., Jiang, Y., Yang, H.** Study on the Phase Change Thermal Storage Performance of Palmitic Acid/Carbon Nanotubes Composites *Composites Part A: Applied Science and Manufacturing* 77 2015: pp. 50 – 55.
http://dx.doi.org/10.1016/j.compositesa.2015.06.020
27. **Fang, G., Li, H., Cao, L., Shan, F.** Preparation and Thermal Properties of Form-stable Palmitic Acid/Active Aluminum Oxide Composites as Phase Change Materials for Latent Heat Storage *Materials Chemistry and Physics* 137 (2) 2012: pp. 558 – 564.
http://dx.doi.org/10.1016/j.matchemphys.2012.09.058
28. **Wang, S., Qin, P., Fang, X., Zhang, Z., Wang, S., Liu, X.** A Novel Sebacic Acid/Expanded Graphite Composite Phase Change Material for Solar Thermal Medium-temperature Applications *Solar Energy* 99 2014: pp. 283 – 290.
http://dx.doi.org/10.1016/j.solener.2013.11.018
29. **Li, D., Cheng, X., Li, Y., Zou, H., Yu, G., Li, G., Huang, Y.** Effect of MOF Derived Hierarchical Co_3O_4/Expanded Graphite on Thermal Performance of Stearic Acid Phase Change Material *Solar Energy* 171 2018: pp. 142 – 149.
http://dx.doi.org/10.1016/j.solener.2018.06.062
30. **Sarı, A., Karaipekli, A., Alkan, C.** Preparation, Characterization and Thermal Properties of Lauric Acid/Expanded Perlite as Novel Form-stable Composite Phase Change Material *Chemical Engineering Journal* 155 (3) 2009: pp. 899 – 904.
http://dx.doi.org/10.1016/j.cej.2009.09.005
31. **Xu, B., Li, Z.** Paraffin/Diatomite Composite Phase Change Material Incorporated Cement-based Composite for Thermal Energy Storage *Applied Energy* 105 2013: pp. 229 – 237.
http://dx.doi.org/10.1016/j.apenergy.2013.01.005
32. **Wang, Y., Xia, T. D., Zheng, H., Feng, H. X.** Stearic Acid/Silica Fume Composite as Form-stable Phase Change Material for Thermal Energy Storage *Energy and Buildings* 43 (9) 2011: pp. 2365 – 2370.
http://dx.doi.org/10.1016/j.enbuild.2011.05.019
33. **Li, M., Guo, Q., Nutt, S.** Carbon Nanotube/Paraffin /Montmorillonite Composite Phase Change Material for Thermal Energy Storage *Sol Energy* 146 2017: pp. 1 – 7.
http://dx.doi.org/10.1016/j.solener.2017.02.003
34. **Sarı, A., Alkan, C., Altıntaş, A.** Preparation, Characterization and Latent Heat Thermal Energy Storage Properties of Micro-nanoencapsulated Fatty Acids by Polystyrene Shell *Applied Thermal Engineering* 73 (1) 2014: pp. 1160 – 1168.
http://dx.doi.org/10.1016/j.applthermaleng.2014.09.005
35. **Wei, H., Xie, X., Li, X., Lin, X.** Preparation and Characterization of Capric-Myristic-Stearic Acid Eutectic Mixture/Modified Expanded Vermiculite Composite as A Form-stable Phase Change Material *Applied Energy* 178 2016: pp. 616 – 623.
http://dx.doi.org/10.1016/j.apenergy.2016.06.109